Available online at www.sciencedirect.com
ScienceDirect
International Journal of Heat and Mass Transfer 50 (2007) 4668–4677
International Journal of HEAT and MASS TRANSFER
www.elsevier.com/locate/ijhmt

Mixing effect on the enhancement of the effective thermal conductivity of nanoparticle suspensions (nanofluids)

C.H. Li [a], G.P. Peterson [b,*]

[a] Department of Mechanical Aerospace, and Nuclear Engineering, Rensselaer Polytechnic Institute, Troy, NY 12180, USA
[b] Department of Mechanical Engineering, University of Colorado, Boulder, CO 80309-0017, USA

Received 22 June 2006; received in revised form 5 March 2007
Available online 23 May 2007

Abstract

In the last decade, a number of investigations have been conducted to identify the possible mechanisms that contribute to the enhanced effective thermal conductivity of nanoparticle suspensions (nanofluids). The Brownian motion of the nanoparticles in these suspensions is one of the potential contributors to this enhancement and the mechanisms that might contribute to this are the subject of considerable discussion and debate. In the current investigation, the mixing effect of the base fluid in the immediate vicinity of the nanoparticles caused by the Brownian motion was analyzed, modeled and compared with existing experimental data available in the literature. The simulation results indicate that this mixing effect can have a significant influence on the effective thermal conductivity of nanofluids.

Keywords: Effective thermal conductivity; Nanoparticle suspensions; Nanofluids; Brownian motion

1. Introduction

Extremely high heat fluxes present a continuing challenge for a wide variety of high technology applications, including memory and CPU chip design [1], micro electromechanical systems (MEMS), chip based lasers, and other novel applications [2,3]. Nanoparticle suspensions (nanofluids) produced by dispersing nanoparticles into normal heat transfer base fluids, such as water or ethylene glycol may present a potential solution to some of these applications [4].

An increasing number of experimental investigations have demonstrated that nanofluids can dramatically increase the effective thermal conductivity of the base fluid [5–18]. Because of the excellent stability of these fluids, nanofluids present a promising alternative to traditional heat transfer fluids in a wide variety of applications. However, the precise mechanisms that contribute to the observed enhancement are not currently well-understood and no widely accepted explanations have been identified. As a result, in order to fully understand the mechanisms that govern the enhancement of these nanofluids and optimize the thermophysical properties, the mixing effect of the base fluid in the immediate vicinity of the nanoparticles caused by the Brownian motion of the nanoparticles was analyzed, modeled and compared with existing experimental data available in the literature.

The earliest explanation of the mechanisms contributing to the enhanced effective thermal conductivity of nanoparticle suspensions was proposed by Maxwell [19], which is for non-interacting particles and non-moving particles, and consisted of an approximation based upon the relative thermal conductivity of the combination of the particle and base fluid. The resulting equation has been successfully applied to predict the effective thermal conductivity of a wide range of particle and fluid/solid matrices, primarily for particles in the millimeter or micro size range. Other investigators have developed a number of equations based on Maxwell's original work, for different particle shapes,

* Corresponding author. Tel.: +1 303 492 8908; fax: +1 303 492 8866.
E-mail address: Bud.Peterson@Colorado.edu (G.P. Peterson).

0017-9310/$ - see front matter © 2007 Elsevier Ltd. All rights reserved.
doi:10.1016/j.ijheatmasstransfer.2007.03.015

that have resulted in more accurate predictive techniques [20–41]. While the Maxwell approximation technique, yields accurate results for suspensions in which the particle sizes are in the range of a millimeter or larger, the accuracy of the models diminishes as the particle size decreases. This is not entirely unexpected since, very few of the equations mentioned above, with the exception of the Maxwell–Garnett model [40,41], include the effect of the particle size on the effective thermal conductivity. In addition, none of these early models included the influence of the Brownian motion of the particles on the properties of the base fluid. It is clear that the particle size is an important factor in the enhancement of the effective thermal conductivity of nanofluids, and that the effect of the particle size increases as the particle size decreases [42]. This is complicated by the fact that the byproduct of stability control, i.e., things like pH, may introduce changes in the rheologic and thermal properties of the nanofluids. Of course, the aggregation and sedimentation of the nanoparticles will also significantly influence the behavior of the nanofluids.

Based on the mechanisms mentioned above, a number of new models have been developed. These newer models, which incorporate the effect of the Brownian motion are based on a combination of Maxwell's equation and the effect of the Brownian motion [43–45], others are based solely on the Brownian motion effect [46], and still others are based on other possible mechanisms, such as a combination of adsorption, Maxwell's equations and the Brownian motion effect [47].

Due to the lack of experimental tools required to isolate the effect of each of these mechanisms, many investigations have focused only on the effects of the Brownian motion of the nanoparticles, using either numerical simulation or experimental techniques [14,16–18,48–51]. There are, however, inconsistent results from both methods, and inconstant results, that result from the dynamic and molecular dynamic simulation of the Brownian motion alone [49,50]. Some of the molecular simulations have concluded that the Brownian motion of the nanoparticles has no impact on the effective thermal conductivity of the nanofluids [50], while, the experimental study of the diffusion of nanofluids provides some evidence of the contribution of the Brownian motion effects, along with other factors [16–18,51]. In order to better understand the governing phenomena and to determine the contribution of the Brownian motion, a numerical simulation was conducted to determine the validity of the previously stated conclusions.

2. Inconsistencies in the simulation and experimental results

Very early in the study of nanofluids, a numerical simulation was conducted to investigate the role of the relative motion between the fluid and the particles, due to the non-affine motion of particles in a mono-dispersed suspension, on the effective thermal conductivity [48]. In this simulation, single spherical particles were divided into identical cubic or spherical cells with each particle occupying one cell [48]. It was assumed that the temperature gradient across the cell was the same as the macroscopic temperature gradient, and that the motion of the fluid was in the opposite direction of the particle motion. The results indicated that microconvection can play a significant role in the overall heat transfer at the macroscopic scale, especially in the volume fraction range of 10–30%. For example, the enhancement could be up to 100% greater when compared to the pure fluid.

Recently, a Brownian dynamics simulation was used to determine the effective thermal conductivity of nanofluids [49]. In this simulation, the *Langevin* equation of motion was used to describe the particle movement and the effect of solvent molecules and was represented by a combination of random forces and frictional terms. The potential energy between the two particles was described by an exponential model as:

$$\Phi_{ji} = A \exp\left[-B\frac{|r_{ji}| - d}{d}\right] \tag{1}$$

where d is the particle diameter, A and B are the parameters for the system, and r_{ji} is the distance between particles j and i. The simulation results agreed with the experimental results reasonably well and demonstrated that the Brownian motion of the nanoparticle is a key factor contributing to the enhanced thermal conductivity of the fluids.

More recently, a molecular dynamics simulation was implemented to study the effects of the Brownian motion of the nanoparticles on the enhancement of the effective thermal conductivity of the nanofluids [50]. This approach utilized kinetic theory to calculate the contribution to the effective thermal conductivity. To determine the contribution of the nanoparticle, the base fluid was assumed to be dragged along with the nanoparticle. The thermal conductivity was represented as:

$$k_B = D_B c_p \tag{2}$$

The thermal conductivity of the base fluid was assumed to be the result of the diffusion of the molecules and was represented as:

$$k_F = D_T c_p \tag{3}$$

From this, the enhancement of the thermal conductivity could be calculated as:

$$\frac{k_B}{k_F} = \frac{D_B}{D_F} \tag{4}$$

where k_B is the thermal conductivity, due to the diffusivity of the nanoparticle; k_F is the thermal conductivity, due to the diffusivity of the fluid molecules; D_B is the diffusivity of the nanoparticle, due to the Brownian motion; D_T is the diffusivity of the fluid molecule; and c_p is the specific heat capacity of the fluid molecule.

This approach is similar to that which has been applied to the thermal conductivity of gases, i.e., the enhancement comes from the net displacement of the fluid molecules and

not the mixing effect. As a result, the simulation results did not show the contribution of the Brownian motion effect of the nanoparticles.

Aside from the inconsistency of the simulation results, some of the experimental results also show, directly or indirectly, that the Brownian motion of the nanoparticles plays an important role in the enhancement of the thermal conductivity of nanofluids [51].

Tests of the effective thermal conductivity of Al_2O_3/DI water and CuO/DI water nanofluids demonstrated a strong dependence on the temperature, and the enhancement increased with increases in temperature [16–18]. Given the possible mechanisms proposed, the contribution resulting solely from the high thermal conductivity of the nanoparticle materials should decrease with increases in the temperature, due to the fact that the thermal conductivity of the base fluid will increase with temperature, while the thermal conductivity of the nanoparticle will decrease with temperature. For example, within the range of temperatures evaluated in the current experiments, the bulk thermal conductivity of Al_2O_3 decreases with increasing temperature, from 0.4144 W/cm K at 0 °C to 0.3103 W/cm K at 100 °C, while the thermal conductivity of pure water increases with increasing temperature, from 0.0057 W/cm K at 0 °C to 0.0067 W/cm K at 100 °C, and the normalized enhancement of effective thermal conductivity of nanofluids increases with temperature with regard to the thermal conductivity of water at each temperature [42]. The intensity of the Brownian motion has a positive square root relationship with temperature, which implies that Brownian motion could contribute to the enhanced thermal conductivity.

Another study that evaluated the relationship between the change of thermal conductivity enhancement and the sample sonication time and aggregation of nanoparticles, indicated that the longer the sonication time, the less aggregation occurred and hence, the higher the resulting enhancement. In addition, following sonication, the longer the elapsed time before testing, the worse the enhancement [16,17]. Because within certain limitations, there is little or no sedimentation, the contribution from the high thermal conductivity of the nanoparticle material should remain the same, however, after the clusters are formed, the intensity of the Brownian motion gets weaker, due to the inverse proportion between the level of Brownian motion and the cluster size.

Still another recent report indicated that the mixing effect of the nanoparticle Brownian motion could enhance the thermal conductivity of nanofluids [51]. In this experimental investigation, a drop of dye in pure water diffuses much more slowly than the same drop of dye in Al_2O_3/water nanofluids. It was also determined that the optimal volume fraction for the diffusion is around 0.5%. These results would appear to provide significant evidence of the effect of the Brownian motion on the enhanced thermal conductivity of nanofluids.

3. Simulation on Brownian motion effect of effective thermal conductivity

Visual observations of the Brownian motion indicate that each nanoparticle can be modeled as having a local periodic motion within the suspension, as shown in Fig. 1. As illustrated, point A and C can be used to represent the farthest points of local periodic motion, and point B is the location at which the local periodic motion has the highest velocity. Based upon this diagram, the velocity and range of influence can be determined from the following expressions as

$$m\frac{d^2x}{dt^2} + bx = 0 \tag{5}$$

or

$$\frac{d^2x}{dt^2} + \omega^2 x = 0, \quad \omega = \sqrt{\frac{b}{m}} \tag{6}$$

$$x(t) = x_0 \cos \omega t + v_0/\omega \sin \omega t \tag{7}$$

where m is the mass, x is the displacement, t is the time, b is a constant, ω is the angular velocity, v_0 is the viscosity, and x_0 is the initial location.

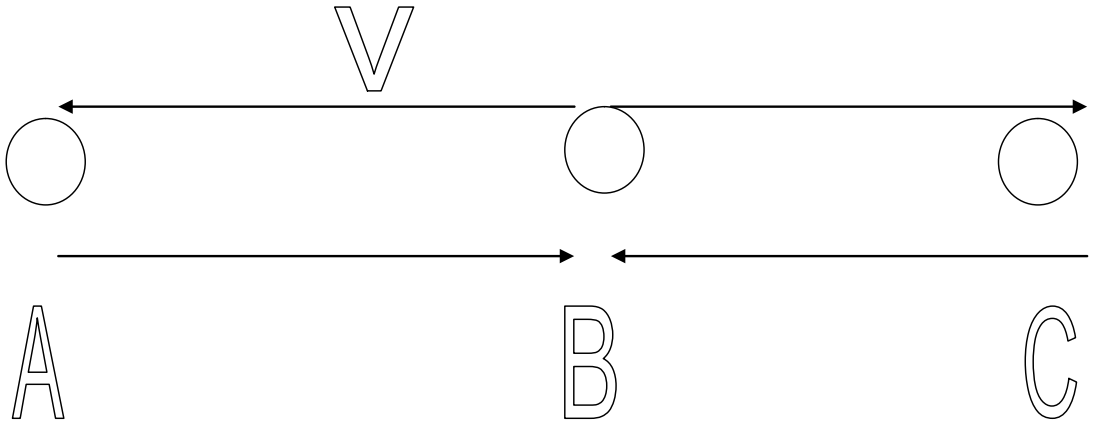

Fig. 1. The local periodic motion of a single nanoparticle.

The range of influence for this local periodic motion model can be calculated and the governing equations for the convection caused by the motion of the nanoparticles in three-dimensional form can be determined as shown below:

Continuity:

$$\frac{\partial \rho}{\partial \tau}+\frac{\partial u}{\partial x}+\frac{\partial v}{\partial y}+\frac{\partial w}{\partial z}=0 \tag{8}$$

Momentum:

$$\rho\left(\frac{\partial u}{\partial \tau}+u\frac{\partial u}{\partial x}+v\frac{\partial u}{\partial y}+w\frac{\partial u}{\partial z}\right)=F_x-\frac{\partial p}{\partial x}+\mu\left(\frac{\partial^2 u}{\partial x^2}+\frac{\partial^2 u}{\partial y^2}+\frac{\partial^2 u}{\partial z^2}\right) \tag{9}$$

$$\rho\left(\frac{\partial u}{\partial \tau}+u\frac{\partial v}{\partial x}+v\frac{\partial v}{\partial y}+w\frac{\partial v}{\partial z}\right)=F_y-\frac{\partial p}{\partial y}+\mu\left(\frac{\partial^2 v}{\partial x^2}+\frac{\partial^2 v}{\partial y^2}+\frac{\partial^2 v}{\partial z^2}\right) \tag{10}$$

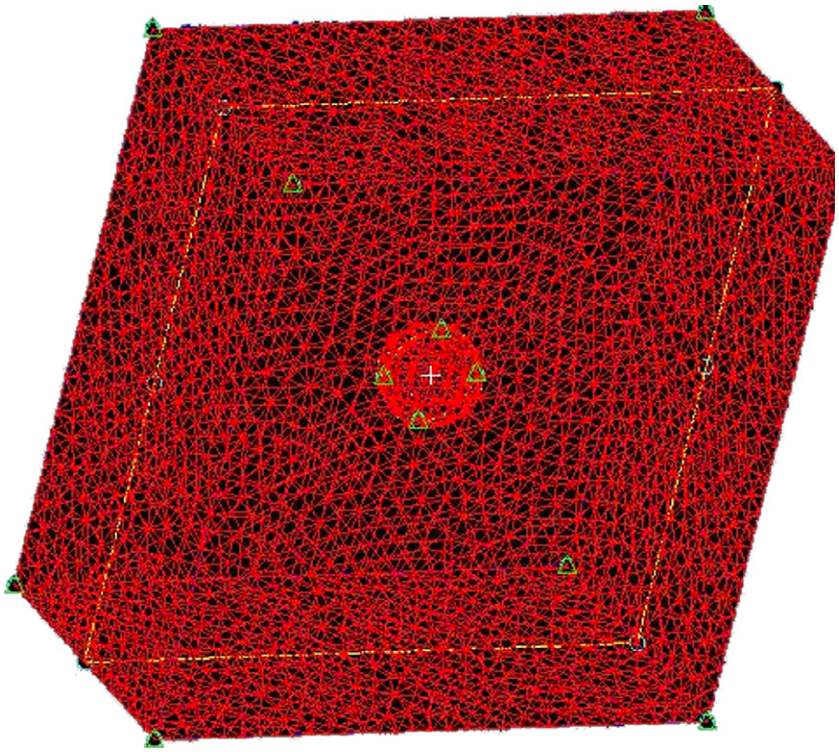

Fig. 2. The mesh generated for the single nanoparticle.

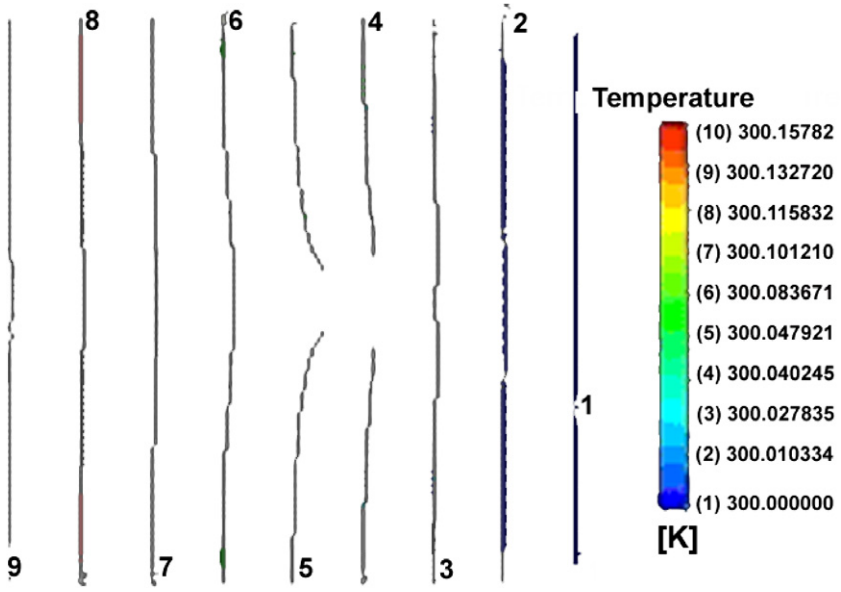

Fig. 3. The simulated temperature field around a single nanoparticle.

$$\rho\left(\frac{\partial w}{\partial \tau}+u\frac{\partial w}{\partial x}+v\frac{\partial w}{\partial y}+w\frac{\partial w}{\partial z}\right)=F_z-\frac{\partial p}{\partial z}+\mu\left(\frac{\partial^2 w}{\partial x^2}+\frac{\partial^2 w}{\partial y^2}+\frac{\partial^2 w}{\partial z^2}\right) \tag{11}$$

Energy:

$$\rho c_p\frac{dT}{d\tau}=\frac{\partial}{\partial x}\left(k\frac{\partial T}{\partial x}\right)+\frac{\partial}{\partial x}\left(k\frac{\partial T}{\partial x}\right)+\frac{\partial}{\partial x}\left(k\frac{\partial T}{\partial x}\right)+\alpha_V T\frac{dp}{d\tau}+\mu\Phi \tag{12}$$

where ρ is the density, u, v, w, and F_x, F_y, F_z are the velocity components and external forces in the x, y, z directions, p is the static pressure, c_p is the specific heat capacity, T is the temperature, k is the thermal conductivity, α_V is the expansion coefficient, μ is the viscosity, and Φ is the diffusion matrix.

This model was generated using CFX 5.5.1 software [52] (a computational fluid dynamics software of British AEA Technology Inc.) on a Pentium-III personal computer. The size of the particle was enlarged from the nanometer to the micron scale, due to the limitations of the software, and a similitude method was used to ensure the validity of the simulation results, which includes the geometrical similarity, the spherical geometry, Kinematic similarity, *Re*, and thermodynamic similarity [53].

The properties of the matter used, were selected from standard figures available from the CFX software. The side boundary surfaces and the surface of the nanoparticles were assumed to be adiabatic, except the left heated surface, which was assumed to have a constant heat flux of 1499.6 W/m^2 and the right isothermal surface, which had a fixed temperature of 300 K (27 °C), as shown in Fig. 6. For the purpose of the parametric study, the initial temperature of the water, $T_{bulk,water}$, was set at 300 K (27 °C). The velocity of 0.01 m/s was adopted for the nanoparticles, which was the same as the previous study [54].

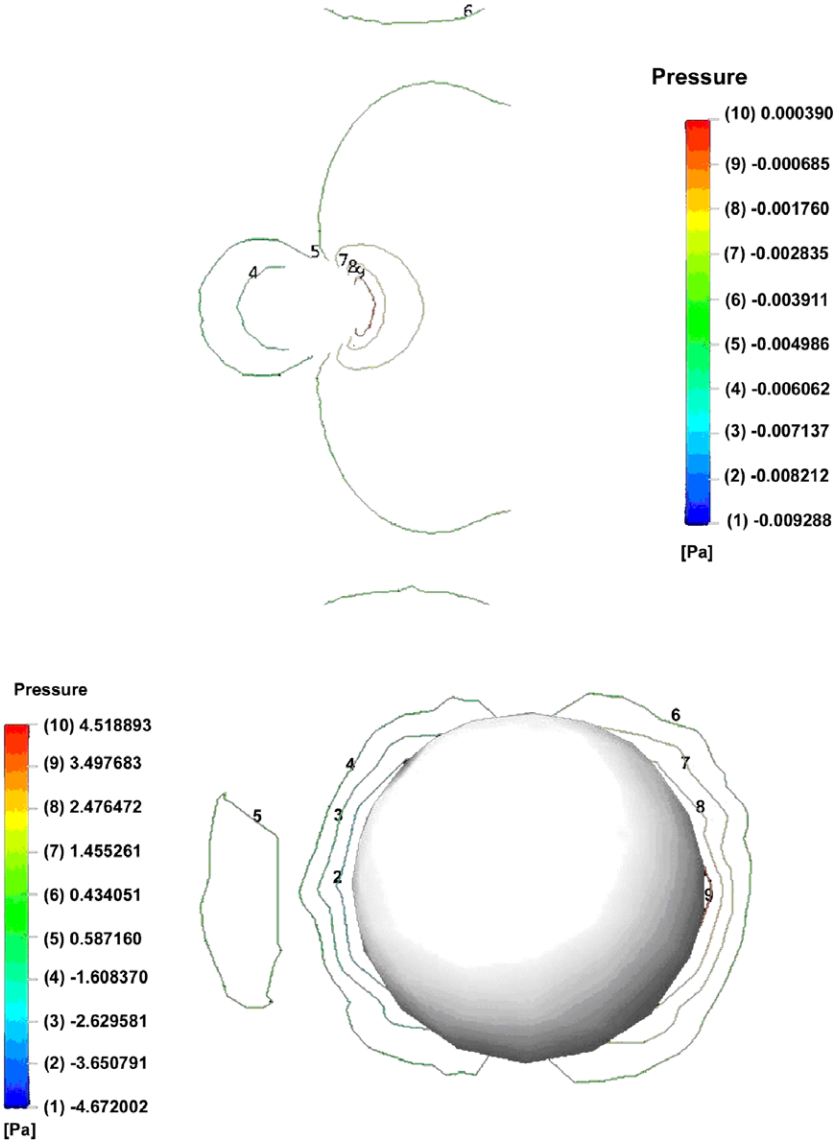

Fig. 4. The simulated relative pressure field around a single nanoparticle at different moving stages.

Initially a single nanoparticle case was studied along with the isothermal, pressure and velocity fields were imaged. Then, the difference between a single nanoparticle and two adjacent nanoparticles was studied, and finally the multi-particle case was investigated.

3.1. Single nanoparticle case

In Fig. 2, the mesh was generated with 3.4×10^5 mesh elements. The nanoparticle had a diameter of 27 nm including the possible adsorption layer [13] which is the actual regime for mutual interaction between the liquid molecules and the nanoparticle surface. The cube domain volume was $300 \times 300 \times 150$ nm. For this model, the transient state was modeled using a time step of 1×10^{-5} s and a total time of 0.01 s. The actual time needed to compute the total time 0.01 s was approximately 48 h in order to achieve a convergent steady-state solution. A refined grid analysis may have resulted in a greater refinement of the mesh in the region of nanoparticles, but current grid appeared to have the enough accuracy for this single nanoparticle study case.

Fig. 3 illustrates the typical simulated temperature field around a nanoparticle after the first stage of modeling. As indicated, the isotherms began to break apart in places

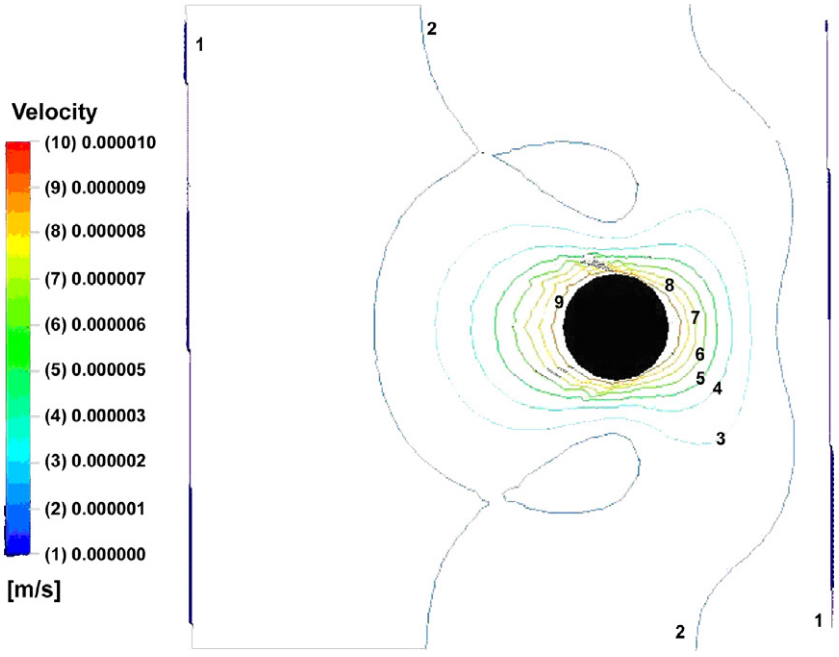

Fig. 5. The velocity field of single nanoparticle simulation.

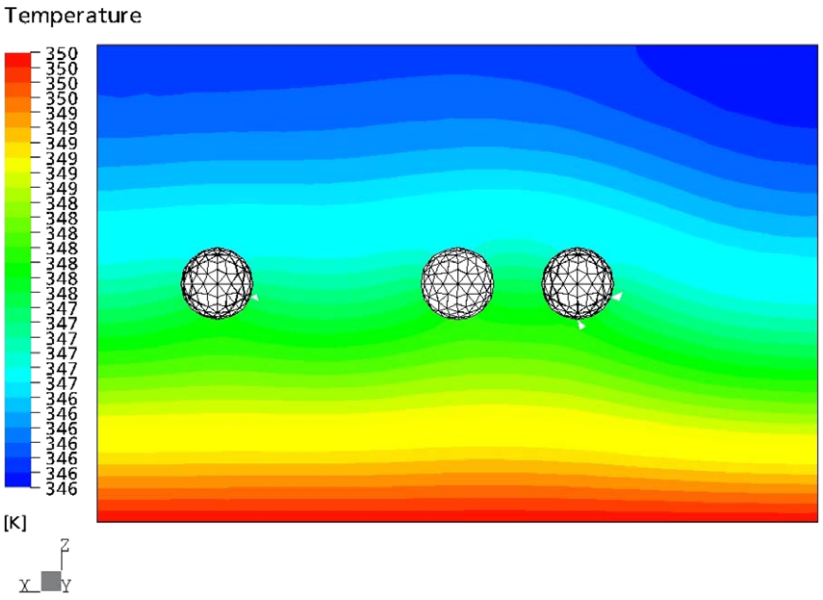

Fig. 6. The comparison for simulated temperature fields around single nanoparticle and two adjacent nanoparticles.

where they contact the nanoparticles and bend along the direction of the nanoparticle movement. As the nanoparticle surface was treated as adiabatic, the curvature of the isotherm was caused by the micro convection induced by the Brownian motion of the nanoparticle.

The pressure field at the top of Fig. 4 shows that the pressure in front of the nanoparticle increases very quickly and the pressure difference between the region behind and in front of the nanoparticle is approximately 9 Pa, with the pressure gradient in front of the nanoparticle, larger than behind the nanoparticle. The bottom one of Fig. 4 shows that at the farthest point of the local periodic motion, the pressure difference between the front and back of the nanoparticle is approximately 0.01 Pa, but that the area of influence is considerably larger than at the beginning of the local periodic motion.

Fig. 5 illustrates the velocity field, which shows a much greater influence in front of the particle than behind it, similar to the pressure field. It is interesting to note that the induced flow velocity gradient is considerably larger in front and behind the nanoparticle than as compared to the velocity gradient above and below the nanoparticle. The most interesting aspect of the velocity field is the area slightly farther away from the nanoparticle. When two nanoparticles are close to each other, the influence on the area will be more than doubled due to the hydrodynamic interaction. This, in turn, increases the heat transfer capacity of the nanofluid in the macroscale.

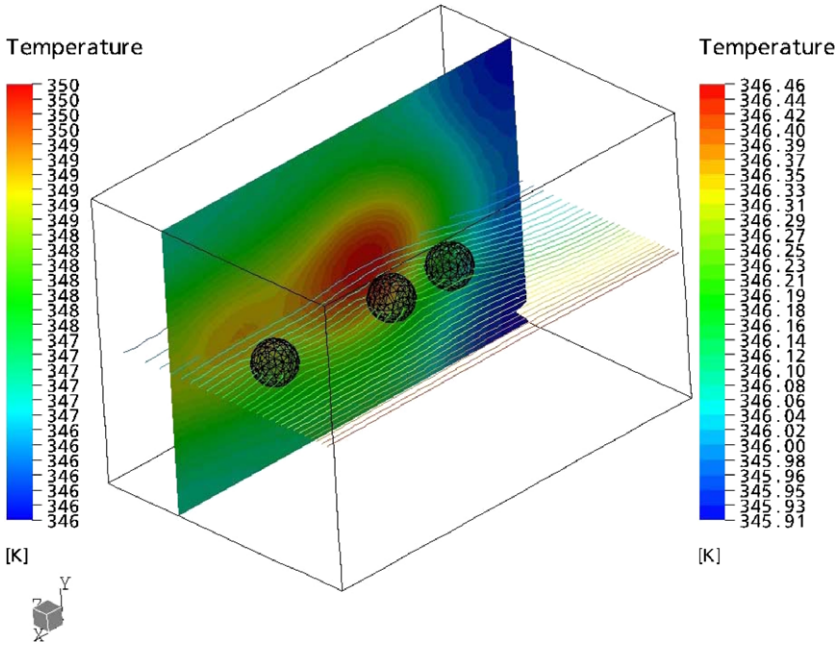

Fig. 7. The comparison for simulated temperature field vertical plane (left, the temperature of X–Z plane; right, the temperature of X–Y plane).

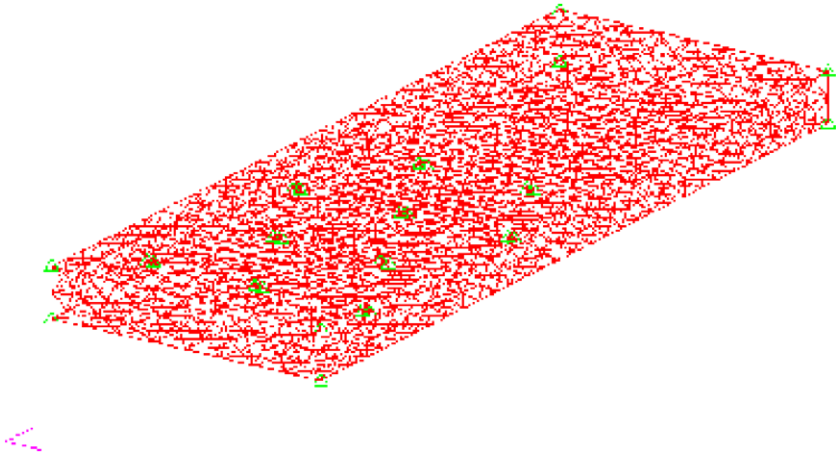

Fig. 8. The mesh generated for modeling multiple nanoparticles.

3.2. Comparison of one and two adjacent nanoparticles effects

The modeling of two adjacent nanoparticles clarifies how the induced micro convection influences the heat transfer capability. The details of the isothermal field are shown in Figs. 6 and 7 and discussed below. In the plane parallel to the moving direction of the nanoparticles, the isotherms around two adjacent nanoparticles are compared to that around a single nanoparticle as shown in Fig. 6. Here, as illustrated, the isotherms reach a maximum over the two adjacent nanoparticles, i.e. the Brownian motion influence is more prominent for multiple nanoparticles.

In the plane perpendicular to the direction of the temperature gradient, the highest temperature appears very close to the two adjacent nanoparticles, then reduces slightly to the other area of the plane as shown in Fig. 7. The temperature of the area right in front of the two adjacent nanoparticles are the highest, which means the hydrodynamic interaction between the nanoparticles greatly enhances the thermal transport capability beside the nanoparticles, not only in front, but also, behind the nanoparticles. It is also apparent that two adjacent nanoparticles in close proximity will have a greater influence on the temperature field than two single nanoparticles, far apart from each other, due to the interaction.

3.3. Effect of multiple nanoparticles

The macro effect of multiple nanoparticles on the thermal conductivity of suspensions, with each nanoparticle considered having local periodic motion and an even distribution of the nanoparticles in the suspension is illustrated in Fig. 8.

Fig. 8 illustrates ten nanoparticles and the mesh is generated angularly with a maximum edge length of 40 nm and 340,000 mesh elements. Every nanoparticle in this model has a diameter of 27 nm including the adsorption layer. The cube domain volume is $200 \times 200 \times 2800$ nm. Three models were used in this simulation to test the effects of the variations of local periodic motion nanoparticles. For each model, transient runs, which required a time step of 1×10^{-5} s and a total time of 0.01 s, were reported every 5×10^{-5} s. The actual time needed to achieve a convergent steady-state solution was approximately 60 h. The extra time spent on this case was the result of a refinement of

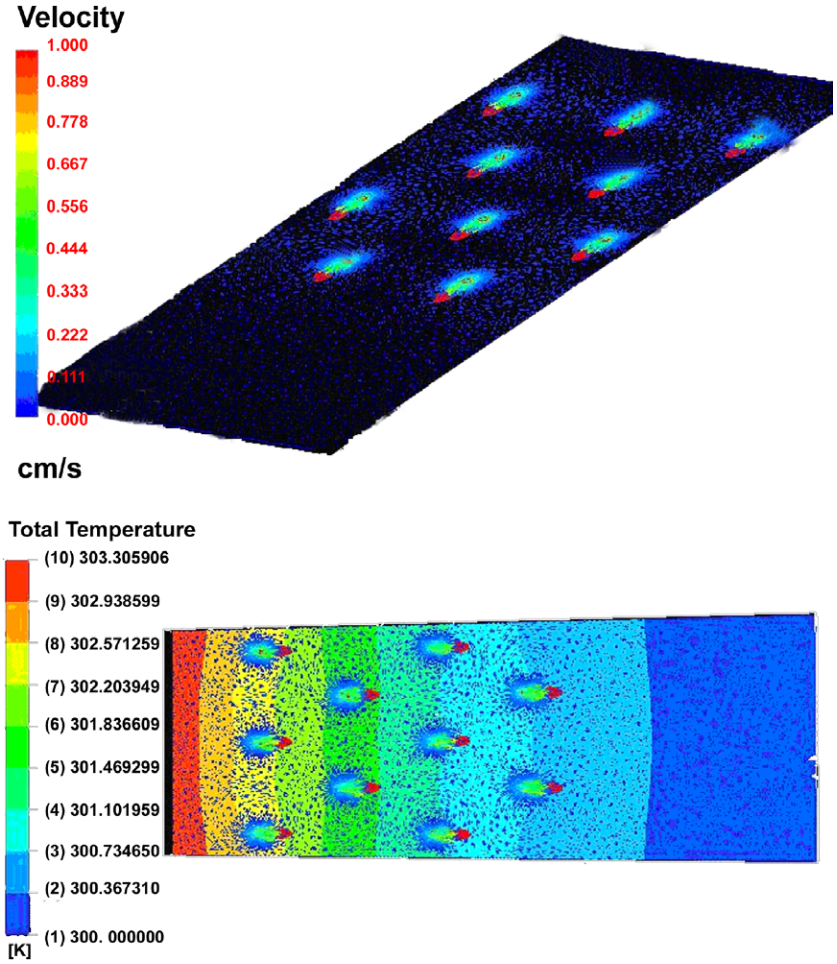

Fig. 9. The velocity and temperature fields of multiple nanoparticles (upper, only velocity fields; lower, combination of velocity and temperature fields).

the mesh in the region of the nanoparticles. These 10 nanoparticles were set to start moving simultaneously with the same velocity, same direction and same life cycle by setting the movement this way, we also tried to illustrate the potential of using an external field to control the speed and movement range of nanoparticles, thereby to control the effective thermal conductivity of nanofluids.

Fig. 9 illustrates a non-parallel isothermal pattern of the temperature distribution. As shown, the temperature gradient is much smaller than that in the pure fluid. The isothermal regions with the nanoparticles are wider than the regions without nanoparticles, and the isothermal regions with more nanoparticles are wider than the regions with fewer nanoparticles. In addition, the isotherms behind the nanoparticle are influenced more heavily than those in front of the nanoparticle. Fig. 9 also illustrates the corresponding velocity field. Here, the micro convection around each nanoparticle and the region it influences are very clear. In this case, the nanoparticles are far away from each other, which implies a volume fraction smaller than 0.1%. In the bottom image of Fig. 9, both velocity and temperature fields are illustrated. In the regions close to the nanoparticles the velocity contours are apparent and even though the distance between the nanoparticles is relatively large, it is still clear that the heat transfer was enhanced as shown by the curved isotherms. All of these observations illustrate the existence and effect of microconvection (the mixing effect of nanoparticle Brownian motion) which serves to greatly enhance the effective thermal conductivity of nanofluids.

4. Conclusions

The corresponding temperature, pressure and velocity fields were simulated using CFX 5.5.1 software and a finite-volume algorithm. The simulations for single, adjacent and multiple nanoparticles were discussed in detail. The results clearly indicate that micro convection/mixing induced by the Brownian motion of the nanoparticles could significantly affect the macro heat transfer capability of the nanofluids. This information, is especially interesting when coupled with other work on the variation of the viscosity of nanofluids, due to the Brownian motion hydrodynamic interaction between nanoparticles [55–61]. The results, clearly indicate the effect of the micro convection/mixing caused by the Brownian motion of nanoparticles in these types of suspensions and demonstrates that the Brownian motion is one of the key factors behind the observed high effective thermal conductivity of nanofluids.

Further investigation of the transport phenomena should be directed at experimental validation and theoretical quantification of the heat transfer enhancement caused by this micro convection/mixing effect, and other possible mechanisms, such as the impact of the adsorbed fluid layer, cluster formation, and thermophysical property changes resulting from the size effect and clustering.

Acknowledgement

The authors acknowledge the support of the National Science Foundation through Grant CTS-0312848.

References

[1] R. Prasher, Applications of Nanotechnology in Electronics Cooling, Seminar, Troy, New York, March 17, 2006.
[2] S.P. Lee, U.S. Choi, Applicaton of metallic nanoparticle suspensions in advanced cooling sytems, in: Y. Kwon, D. Davis, H. Chung, (Eds.), Recent Advances in Solids/Structures and Application of Metallic Materials, The American Society of Mechanical Engineers, New York, PVP-Vol 342/MD-Vol 72, 1996, pp. 227–234.
[3] J.B. Gordon, Nanofluids: rheology and its implication on heat transfer, Private seminar, MIT, Boston, April 20th, 2006.
[4] S.U.S. Choi, Enhancing thermal conductivity of fluids with nanoparticles, in: D.A. Siginer, H.P. Wang (Eds.), Developments and Applications of Non-Newtonian Flows, American Society of Mechanical Engineers, New York, 1995.
[5] J.A. Eastman, S.U.S. Choi, S. Li, L.J. Thompson, S. Lee, Enhanced thermal conductivity through the development of nanofluids, Nanophase Nanocompos. Mater. II (1997) 3–11.
[6] S. Lee, S.U.S. Choi, S. Li, J.A. Eastman, Measuring thermal conductivity of fluids containing oxide nanoparticles, Trans. ASME 121 (May) (1999) 280–289.
[7] J.A. Eastman, S.U.S. Choi, S. Li, W. Yu, L.J. Thompson, Anomalously increased effective thermal conductivities of ethylene glycol-based nanofluids containing copper nanoparticles, Appl. Phys. Lett. 78 (6) (2001) 718–720.
[8] Y. Xuan, Q. Li, Heat transfer enhancement of nanofluids, J. Eng. Thermophys. 20 (4) (2000) 465–470 (Chinese).
[9] Y. Xuan, Q. Li, Heat transfer enhancement of nanofluids, Int. J. Heat Fluid Flow 21 (2000) 58–64.
[10] H. Xie, J. Wang, T. Xi, Y. Liu, F. Ai, Dependence of the thermal conductivity of nanoparticle–fluid mixture on the base fluid, J. Mater. Sci. Lett. 21 (2002) 1469–1471.
[11] H. Xie, J. Wang, T. Xi, Y. Liu, F. Ai, Thermal conductivity enhancement of suspensions containing nanosized alumina particles, J. Appl. Phys. 91 (7) (2002) 4568–4572.
[12] X. Wang, X. Xu, U.S. Choi, Thermal conductivity of nanoparticle–fluid mixture, J. Thermophys. Heat Transfer 13 (4) (1999) 474–480.
[13] B.X. Wang, H. Li, X.F. Peng, Research on the heat-conduction enhancement for liquid with nanoparticle suspensions, J. Therm. Sci. 11 (3) (2002) 214–219.
[14] S.K. Das, N. Putra, P. Thiesen, W. Roetzel, Temperature dependence of thermal conductivity enhancement for nanofluids, J. Heat Transfer 125 (August) (2003) 567–574.
[15] H.E. Patel, S.K. Das, T. Sundararajan, A.S. Nair, G. Beena, T. Pradeep, Thermal conductivities of naked and monolayer protected metal nanoparticle based nanofluids: manifestation of anomalous enhancement and chemical effects, Appl. Phys. Lett. 83 (14) (2003) 2931–2933.
[16] T.K. Hong, H.S. Yang, Study of the enhanced thermal conductivity of Fe nanofluids, J. Appl. Phys. 97 (2005) 064311.
[17] K.S. Hong, Thermal conductivity of Fe nanofluids depending on the cluster size of nanoparticles, Appl. Phys. Lett. 88 (2006) 031901.
[18] C.H. Li, G.P. Peterson, Experimental investigation of temperature and volume fraction variations on the effective thermal conductivity of nanoparticle suspensions, J. Appl. Phys. 99 (8) (2006) 084314.
[19] J.C. Maxwell, A Treatise on Electricity and Magnetism, third ed., vol. I, Oxford University Press, 1892.
[20] L. Rayleigh, On the influence of obstacles arranged in rectangular order upon the properties of a medium, Philos. Mag. 34 (1892) 481–502.

[21] H. Fricke, A mathematical treatment of the electric conductivity and capacity of disperse systems, Phys. Rev. 24 (1924) 575–587.
[22] R.L. Hamilton, O.K. Crosser, Thermal conductivity of heterogeneous two-component systems, I&EC Fund. 1 (3) (1962) 187–191.
[23] Von D.A.G. Bruggeman, Berechnung verschiedener physikalisher konstanten von heterogenen substanzen, Ann. Phys. 5 (24) (1935) 636–664 (German).
[24] J.B. Keller, Conductivity of a medium containing a dense array of perfectly conducting spheres or cylinders or nonconducting cylinders, J. Appl. Phys. 34 (4) (1963) 991–993.
[25] L.G. Leal, On the effective conductivity of a dilute suspension of spherical drops in the limit of low particle peclet number, Chem. Eng. Commun. 1 (1973) 21–31.
[26] D.J. Jeffrey, Conduction through a random suspension of spheres, Proc. Royal Soc. London A 335 (1602) (1973) 355–367.
[27] A. Rocha, A. Acrivos, On the effective thermal conductivity of dilute dispersions: highly conducting inclusions of arbitrary shape, Quarter. J. Mech. Appl. Math. 26 (4) (1973) 441–455.
[28] A. Rocha, A. Acrivos, On the effective thermal conductivity of dilute dispersions, Quarter. J. Mech. Appl. Math. 26 (2) (1973) 217–233.
[29] G.K. Batchelor, Transport properties of two-phase materials with random structure, Ann. Rev. Fluid Mech. 6 (1974) 227–255.
[30] R.W. O'Brien, A method for the calculation of the effective transport properties of suspensions of interacting particles, J. Fluid Mech. 9 (l) (1979) 17–39.
[31] H. Hatta, M. Taya, Effective thermal conductivity of a misoriented short fiber composite, J. Appl. Phys. 58 (7) (1985) 2478–2486.
[32] R.H. Davis, The effective thermal conductivity of a composite material with spherical inclusions, Int. J. Thermophys. 7 (3) (1986) 609–620.
[33] D.P.H. Hasselman, L.F. Johnson, Effective thermal conductivity of composites with interfacial thermal barrier resistance, J. Compos. Mater. 21 (June) (1987) 508–515.
[34] J.F. Brady, R.J. Phillips, J.C. Lester, G. Bossis, Dynamic simulation of hydrodynamically interacting suspensions, J. Fluid Mech. 195 (October) (1988) 257–280.
[35] R.T. Bonnecaze, J.F. Brady, A method for determining the effective conductivity of dispersions of particles, Proc. Royal Soc. London 430 (1879) (1990) 285–313.
[36] R.T. Bonnecaze, J.F. Brady, The effective conductivity of random suspensions of spherical particles, Proc. Royal Soc. London A 432 (1991) 445–465.
[37] S.Y. Lu, S.T. Kim, Effective thermal conductivity of composites containing spheroidal inclusions, AIChE J. 36 (6) (1990) 927–938.
[38] I.C. Kim, S. Torquato, Effective conductivity of composites containing spheroidal inclusions: comparison of simulations with theory, J. Appl. Phys. 74 (3) (1993) 1844–1854.
[39] S.Y. Lu, H.C. Lin, Effective conductivity of composites containing aligned spheroidal inclusions of finite conductivity, J. Appl. Phys. 79 (9) (1996) 6761–6769.
[40] D.P. Hasselman, L.F. Johnson, Effective thermal conductivity of composites with interfacial thermal barrier resistance, J. Compos. Mater. 21 (1987) 508–515.
[41] C.W. Nan, R. Birringer, D.R. Clarke, H. Gleiter, Effective thermal conductivity of particulate composites with interfacial thermal resistance, J. Appl. Phys. 81 (10) (1997) 6692–6699.
[42] C.H. Li, G.P. Peterson, The effect of particle size on the effective thermal conductivity of Al_2O_3–water nanofluids, J. Appl. Phys. 101 (4) (2007) 044312.
[43] R. Prasher, P. Bhattacharya, P.E. Phelan, Thermal conductivity of nanoscale colloidal solutions (nanofluids), Phys. Rev. Lett. 94 (Jan) (2005) 025901.
[44] C.H. Li, G.P. Peterson, Due role of nanoparticle in the thermal conductivity enhancement of nanoparticle suspension, in: Proceedings of IMECE 2005 ASME International Mechanical Engineering Congress and Exposition, November 5–11 2005, Orlando, Florida.
[45] D.H. Kumar, H.E. Patel, V.R.R. Kumar, T. Sundararajan, T. Praseep, S.K. Das, Model for heat conduction in nanofluids, Phys. Rev. Lett. 93 (14) (2004) 155301.
[46] J. Koo, C. Kleinstreuer, A new thermal conductivity model for nanofluids, J. Nanoparticle Res. 6 (2004) 577–588.
[47] S.P. Jang, S.U.S. Choi, Role of Brownian motion in the enhanced thermal conductivity of nanofluids, Appl. Phys. Lett. 84 (May) (2004) 4316.
[48] S.K. Gupte, S.G. Advani, P. Huq, Role of micro-convection due to non-affine motion of particles in a mono-disperse suspension, Int. J. Heat Mass Transfer 38 (16) (1995) 2945–2958.
[49] P. Bhattacharya, S.K. Saha, A. Yadav, P.E. Phelan, Brownian dynamics simulation to determine the effective thermal conductivity of nanofluids, J. Appl. Phys. 95 (11) (2004) 6492–6494.
[50] W. Evans, J. Fish, P. Keblinski, Role of Brownian motion hydrodynamics on nanofluid thermal conductivity, Appl. Phys. Lett. 88 (2006) 093116.
[51] S. Krishnamurthy, P. Bhattacharya, P.E. Phelan, R.S. Prasher, Enhanced Mass Trans. Nanofluids Nanolett. 6 (3) (2006) 419–423.
[52] C. Greenfield, G.L. Quarini, Look at my particles—they keep sticking to the wall, in: Proceedings of the Third CFX International Users Conference, Larimer House, Chesham, UK, 1996, pp. 443–458.
[53] D.J. Schuring, Scale Models in Engineering, Pergamon Press, Oxford, 1977.
[54] B.X. Wang, H. Li, X.F. Peng, Research on the effective thermal conductivity of nano-particle colloide, in: TED-AJ03-583, 6th AJSME 2003, Hawaii, USA, 2003.
[55] G.K. Batchelor, Brownian diffusion of particles with hydrodynamic interaction, J. Fluid Mech. 74 (1976) 1–29.
[56] J.F. Brady, R.J. Phillips, J.C. Lester, G. Bossis, Dynamic simulation of hydrodynamically interacting suspensions, J. Fluid Mech. 195 (1988) 257–280.
[57] J.F. Brady, The rheological behavior of concentrated colloidal dispersions, J. Chem. Phys. 99 (1) (1993) 567–581.
[58] K. Vondermassen, J. Bongers, A. Mueller, H. Versmold, Brownian motion: a tool to determine the pair potential between colloid particle, Langmuir 10 (1994) 1351–1353.
[59] J.F. Brady, J.F. Morris, Microstructure of strongly sheared suspensions and its impact on rheology and diffusion, J. Fluid Mech. 348 (1997) 103–139.
[60] A.J. Banchio, J. Gapinski, A. Patknowski, W. Haubler, A. Fluerasu, S. Sacanna, P. Holmqvist, G. Meier, M.P. Lettinga, G. Nagele, Many-body hydrodynamic interaction in charge-stabilized suspensions, Phys. Rev. Lett. 96 (2006) 138303.
[61] G.P. Peterson, C.H. Li, in: J.P. Hartnett, T.F. Irvine (Eds.), Advances in Heat Transfer, vol. 39, Pergamon, New York, 2005, pp. 261–392.